PROCEEDINGS, 42nd Workshop on Geothermal Reservoir Engineering
Stanford University, Stanford, California, February 13-15, 2017
SGP-TR-212

Experimental Investigation of Hydraulically Induced Fracture Properties in Enhanced Geothermal Reservoir Stimulation

Lianbo Hu, Ahmad Ghassemi

Reservoir Geomechanics and Seismicity Research Group

The University of Oklahoma, Norman, OK 73019 USA

ahmad.ghassemi@ou.edu

John Pritchett, Sabodh Garg

Leidos Inc.

Keywords: Enhanced geothermal systems, fracture properties, acoustic emission, spontaneous potential, tracer, temperature

ABSTRACT

Geothermal energy production by water circulation in man-made fracture systems is referred to as enhanced or engineered geothermal systems (EGS) production. The permeable zones of an EGS must be created by stimulation, a process which involves fracture initiation and/or activation of discontinuities such as joints by pore pressure and stress perturbations. In this work, we study the hydraulically induced fracture properties on a laboratory scale using acoustic emission (AE) cloud, spontaneous potential (SP), and tracer analysis. To achieve this goal, we have performed reservoir stimulation using 13x13x13 inch^3 pre-heated cubical rock samples under representative in-situ stress regimes. During this stimulation stage and the subsequent production processes, sensors are used on the block surfaces and within cavities and wellbores to characterize and locate acoustic emissions (AE) caused by the stimulation, and to monitor local changes in fluid pressure, temperature and electrical self-potential (SP). Cold water is injected centrally and simultaneously collected from nearby miniature production wells. Water with tracer was injected after the circulation test, and concentrations in fluid collected from the production wells could be measured. The data collected could be then analyzed to develop a better understanding of the fractures and the induced fracture permeability and fluid/heat flow.

1. INTRODUCTION

Geothermal energy is considered to be a promising option for a future clean and sustainable energy supply. However, certain technical barriers need to be removed for large scale utilization of the resources. Particularly, questions related to reservoir creation in different rock types and stress conditions need be addressed, and good characterization of the induced or activated fracture will then provide fundamental information needed to evaluate and then develop the enhanced geothermal system. Laboratory scale studies present a good opportunity to help resolve some of the pending challenges along with recent field-scale efforts within the framework of the FORGE (Frontier Observatory for Research in Geothermal Energy) initiative. The main purpose of this project is to gain a better understanding of the geometry and the heat exchange properties of the hydraulically induced fractures in enhanced or engineered geothermal systems (EGS). To realize this goal, a new lab-scale hydraulic fracture test system has been developed that allows us to replicate aspects of the EGS hydraulic fracturing treatment in the field. Our work improves the state-of-the-art by allowing the simultaneous monitoring of acoustic emission (AE), spontaneous potential (SP) and tracers during the stimulation and circulation phases. In this work, our most recent promising result will be presented and discussed.

2. THE LAB-SCALE EGS TEST SYSTEM

The lab-scale EGS system has several integrated subsystems. The main subsystems are: a polyaxial frame and heaters, hydraulic fracturing and circulation systems, temperature, AE and SP data acquisition systems, and fluids and tracers. Figure. 1 (left) shows the fully assembled test systems. Sensors on the block surfaces and within cavities and wellbores allow us to characterize and locate AE caused by the stimulation and to monitor local changes in fluid pressure, temperature, and SP. The polyaxial frame can be sealed with high pore pressure in the test block and may be pre-heated to simulate a geothermal system. Multiple wells can be drilled into the test block to simulate injection and production. Fluid produced from the production wells can be collected and analyzed. A multiple stage fracturing test was also successfully conducted on this system with independent control on each stage. Figure.1 (right) shows a longitudinal sectional view of the block under test. More information about these subsystems is provided by Hu (2016).

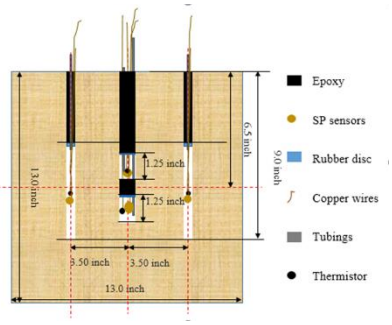

Figure 1: Fully assembled test system and longitudinal sectional view of a two-stage hydraulic fracturing test block.

3. PRELIMINARY TEST RESULTS

3.1 Test Setup

In this section, some promising test results from a 13.0 inch cubical Sierra White granite block will be presented and discussed. Figure. 2 (left) is a top view showing the layout of the wells and the AE sensors on the top surface, and Figure. 2 (right) is a longitudinal sectional view of the sample showing the interior layout of the wells. The injection hole was drilled with a 0.75 inch diameter drill bit. The injection well has a drilled depth of 7.5 inch and a diameter of 0.78 inch. High strength epoxy was poured into the hole to seal the annulus between the injection tubing and the wellbore wall, leaving a 2.0 inch unsealed injection interval at the bottom. Four production wells with depths of 9.0 inch were drilled 3.5 inches away from the injection well and have 5.0 inch unsealed production intervals at the bottom. The diameter of the production wells is 0.4 inch. A thermistor was located at the center of each downhole unsealed interval to measure temperature histories. SP sensors were placed in each well, and the one in the injection well served as the reference electrode. The SP sensors were made by soldering a copper cable to a thin circular copper sheet. Epoxy cylinders with diameter slightly smaller than the wellbores were put inside the wells to occupy space and thus to minimize the effect of wellbore storage. The locations of SP sensors and AE sensors are shown in Figure. 3. The space between the rock block and the inner surface of the loading frame is occupied by flatjacks, PEEK plates and steel plate spacers. After the sample was put into the frame and the frame was fully assembled, principal stresses were applied by injecting oil into the flatjacks to predetermined pressure levels. Since we tried to control the induced fracture within the rock block, the hydraulic fracturing process was conducted carefully and controlled by a LABVIEW program.

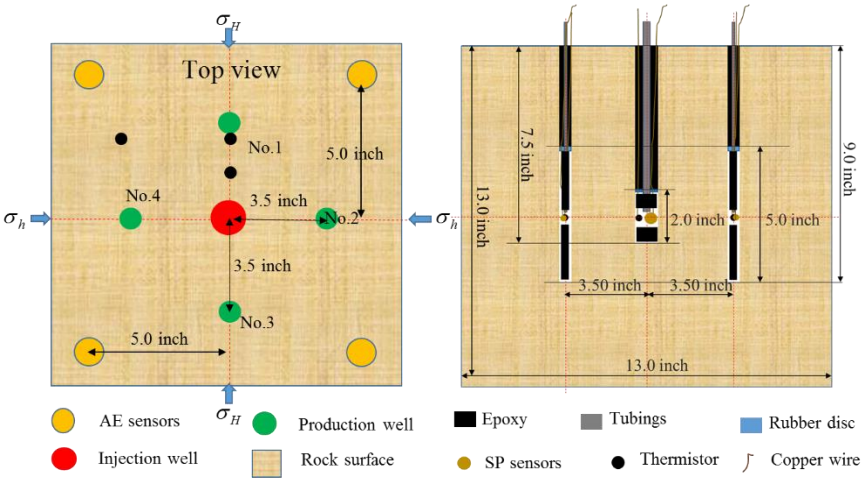

Figure 2: Layout of injection well (left) and production wells with sensors (right)

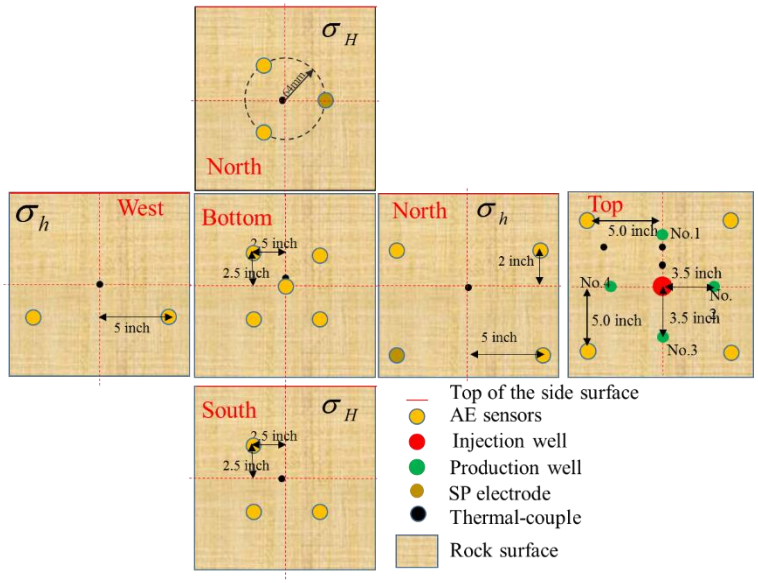

Figure 3: Fold-out diagram of the Sierra White block with AE sensors and SP sensors.

3.2 Test Parameters and Results of the Fracturing Test

At first, hydraulic fracturing test was conducted without fluid in the frame and the stress conditions listed in Table 1. Though we did not saturate the whole block, we tried to saturate the inner part of the block to get the SP response by maintaining the pressure in the wells at a level of 400 psi for eight hours. For better control of the fracture propagation, the injection rate was set to be 2.0 ml/min.

Table 1: Experimental parameters for Sierra White granite block

σ_V , psi	σ_h , psi	σ_H , psi
500	1000	1500

Figure 4 shows the recorded data for the test, namely injection pressure (purple), flow rate (blue), SP response (green, SP1), and accumulation of AE events (dark red). The controlling program reduced the injection rate to 0.02 ml/min right after the pressure drop exceeded the preset value. Ninety seconds later, the injection rate was reset to the initial value and this second injection stage lasted about 52s. Then, pumping ceased. From the test result, it is clear that the injection pressure and the SP response are in proportion to each other. Also, it can be seen that the proportionality factor between SP and pressure is different before and after fracturing. The SP-pressure drop response indicates that electrokinetic mechanism was the main source for the SP. Also, it is clear that the SP response in well No.1 (SP1) is different from that in other production wells. This indicates that production well No.1 was somehow intersected by the induced fracture.

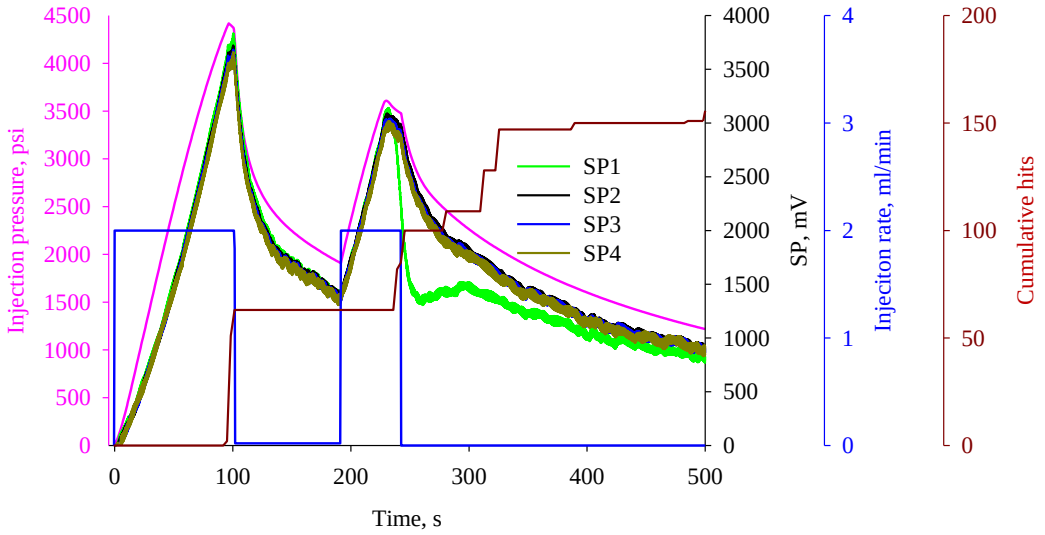

Figure 4: The recording data for Sierra White granite block test.

To provide a better understanding of the relationship between the pressure drop and the SP recording, pressure drop vs SP is plotted in Figure 5, which shows excellent proportionality between pressure drop and SP response. The time interval for the first period of injection is divided into two subintervals: before (0-97s) and after fracturing (97-191s). The electrokinetic coupling coefficient is defined as the ratio of SP to pressure difference (Jouniaux and Pozzi , 1995). For the time interval before fracture, the electrokinetic coupling coefficient has a value is 0.5293 mV/psi (for the initial part) and is 0.9865mV/psi after fracturing (Figure 5), an increase of about 86%. %. This increase of electrokinetic coupling coefficient is caused by the increased permeability at higher pore pressure due to dilatancy of microcracks and the related decreased hydraulic tortuosity. Possible increase of zeta potential of the new fracture surface area also could contribute to the higher proportionality factor (Moore and Glaser, 2007). This also explains why the coupling coefficient increases after the injection pressure exceeds 2000 psi.

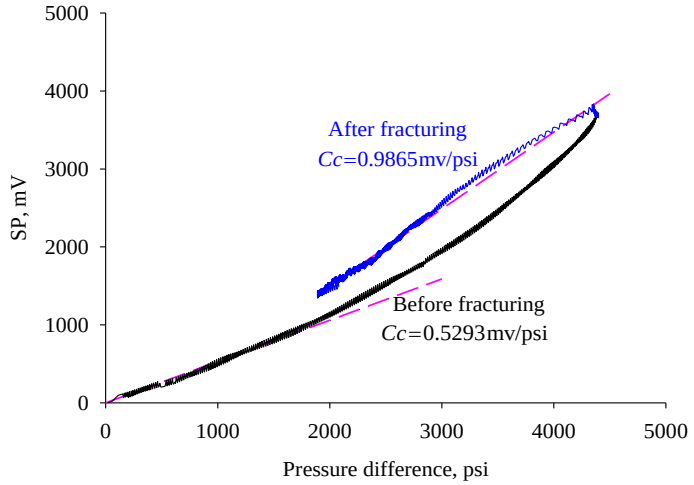

Figure 5: The electrokinetic coupling coefficient for different intervals.

During the fracturing process, all production wells were shut-in and the pressure changes in the wells were recorded and plotted in Figure 6. It can be seen from the figure which production well is connected with the injection well by the induced fracture and which is not. In this case, it is obvious that the production well No.2 was intersected by the induced fracture. Also, we could interpret that after the first period of hydraulic fracturing, the induced fracture propagated toward to well No.1 for a small distance while it did not intersect with the well No.1. After the second period of injection, the well No.2 was fully connected with the injection well by induced fracture.

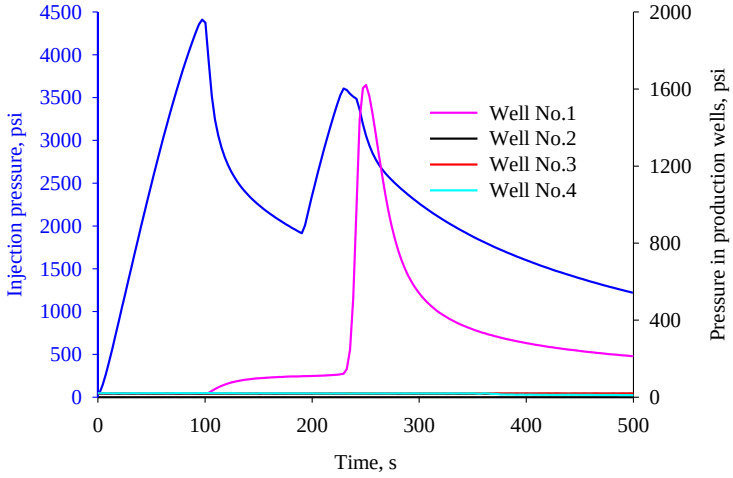

Figure 6: The injection pressure and pressure in production wells.

3.4 Induced Fracture Geometry Based on Acoustic Emission

The breakdown pressure was 4418 psi and the maximum pressure during the second period of injection is 3609 psi. The break down pressure was higher than its theoretical value; wellbore size effects and rock heterogeneity could be the main reasons for this phenomenon. From Figure 4, we notice that during the whole period of the hydraulic fracturing test, only about 150 acoustic emission hits were recorded, and only 15 acoustic events were located based on the time difference when these hits were received by the AE sensors at different location on the block surface. Figure 7 shows the relative location of the AE events and production and injection section in the wells. Though we did not obtain a large number of AE events, the AE cloud in Figure 7 provides a very good indication of the fracture propagation direction and extension and it agrees very well with the pressure behavior in the production wells. In Figure 7, it is clear that well No.1 was intersected by the hydraulically induced fracture. The induced fracture may just follow the weak zone of the granite block and the energy released was relatively low and thus the number of hit received was lower that what was expected.

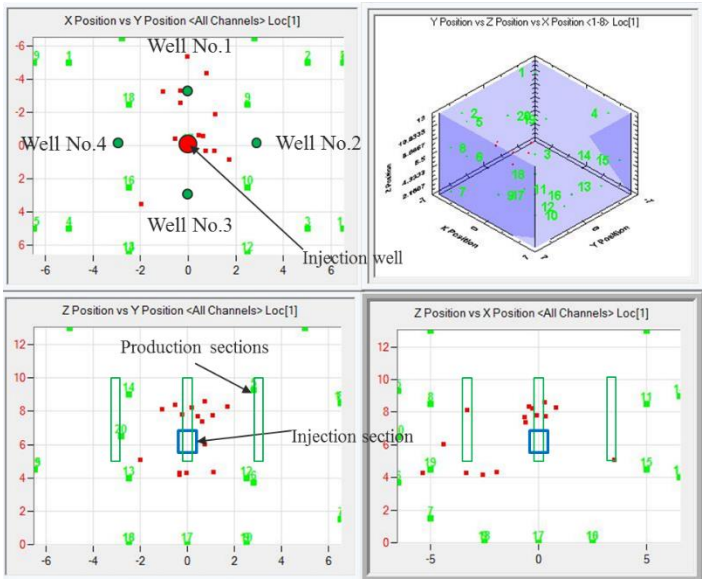

Figure 7: The relative location of the AE events and production and injection section

3.5 Circulation Test Result

After the fracturing stage was completed, 0.002 mole/L sodium chloride solution was poured into the frame and then the heating system was connected to heat the whole polyaxial frame. After about 10 hours of heating, the granite block was heated to a near uniform temperature and then cold 0.002 mole/L sodium chloride solution was injected into the center well. By putting cold packs around the injection pumps and pre-cooling the injection fluid and also placing a long section of the injection tubing into an ice water tank, the temperature of the injection fluid was close to zero Celsius. To prevent the fracture induced during the previous test from propagating during circulation, the injection rate was increased step by step. During the whole period of the circulation test, the pressure at the production wells and the boundary of the granite block was close to atmosphere pressure, since the valves controlling the production were fully open. At the beginning, the injection pressure was as high as 3300 psi with injection rate of 1 ml/min. After the injection rate was increased to 3 ml/min, a peak injection pressure of 3623 psi occurred and then the injection pressure decreased with higher injection rate, this very likely is indicative of a slight propagation of the fracture which resulted in further fracture permeability increases due to the cooling effect and higher pressure in the fracture. Once the injection rate increased to 25 ml/min, a major fracture propagation event occured (a sudden increase of received AE hits is observed on the cumulative AE hit curve) and then the injection pressure dropped to about 1300 psi and then injection pressure increased to about 2300 psi when the injection rate was maintained at 30 ml/min. At the end of the circulation test, the injection pressure was stable at 2330 psi. Some pressure drop or injection rate drop happened during this period caused by the switching of pumps (since the volume capacity of the pump is limited, we had to use two pumps).

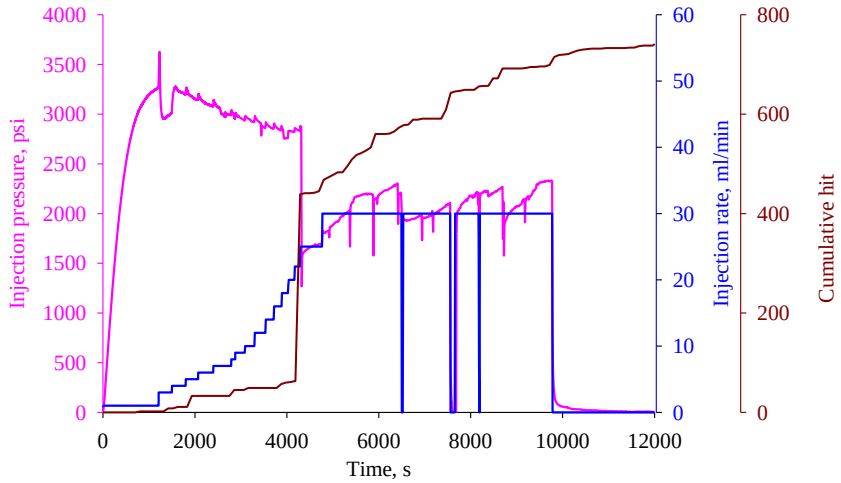

Figure 8: Injection flowrate and pressure, and received cumulative AE hit

During the circulation test, the temperature changes in the wells were also recorded and plotted in Figure 9. When the injection rate was 1 ml/min, the temperature in all the wells remained the same; this is because the injection rate was too small so the injected fluid was heated to the temperature of the rock before it reached the injection section. Temperature in well No.1, which was connected to the injection section after the fracturing test did show a decrease followed by a slight increase. This increase could have resulted from the fact that the thermistor was submerged in water and the water may have contacted the wires due to insufficient sealing, decreasing its

measured resistance. Before the occurrence of the major fracture propagation event during the circulation phase, the temperature in other production wells decreased very slowly. However, after the fracture extension event, the temperature in production wells No.2 and No.3 started to decrease more rapidly. Then, the temperature in these wells started to fluctuate. This can be attributed to the production rate change due to the new fracture becoming available for the fluid to flow, and the injection interruption when the pump was switched. In the last period of the circulation test, the temperature in the wells almost reached a stable level. Just before stopping the circulation, the temperature drop in the injection well was 39.2 ^{o}C. The maximum temperature drop in the production wells was more than 10 ^{o}C. Figure 10 shows the temperature on the block surfaces, from which we notice that the temperature change on most rock surfaces was less than 1.0 ^{o}C. The temperature change on the top surface is higher due to the fact that the injection tubing carrying cold water went into the block through the top surface.

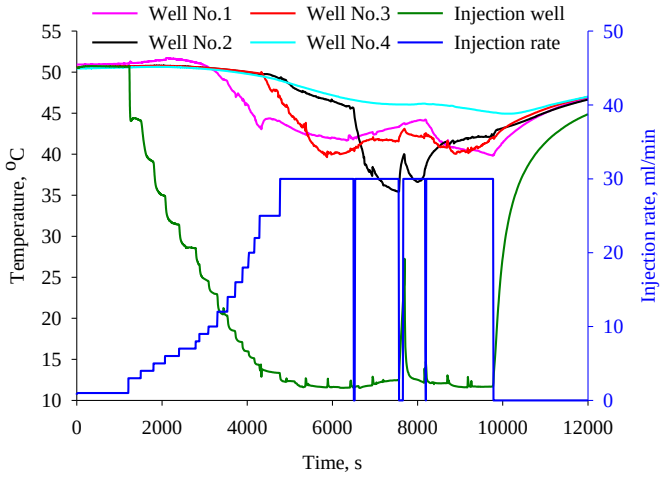

Figure 9: Temperature in the injection well and production wells

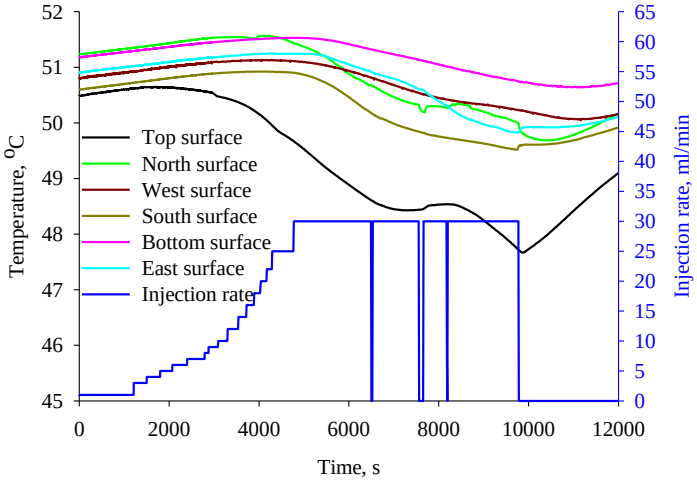

Figure 10: Injection rate and temperature on the block surface

During the circulation test, the fluid produced from the production wells was collected and the production rate of these wells was then calculated based on the volume of the fluid collected. Figure 11 shows the production rate and injection rate. Before the major fracture propagation, most of the fluid was produced from well No.1. After wells No.2 and No.3 were intersected, the production rate in well No.1 dropped substantially. After the fluctuation, the average production rate for wells No.1, No.2 and No.3 were 8.87 ml/min, 5.9 ml/min and 7.46 ml/min respectively (average of the last three measurements). Totally, about 74 percent of the production fluid was produced from the production wells. Almost no fluid was produced from well No.4. It is likely that the rest leaked-off to the surface of the block. The AE cloud in Figure 7 indicates the fracture to be close to the north surface of the block.

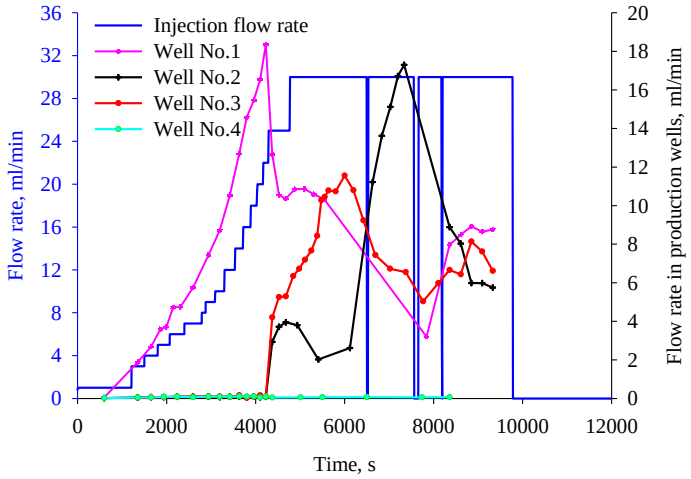

Figure 11: Injection rate and production rate in wells

3. Tracer Test Result

After the circulation test, a tracer test was carried out. During the circulation test, 10.36 ml of 1mole/L (PPM: 58440) sodium chloride solution was first injected at 1 ml/min injection rate and then 0.002 mole/L (PPM: 116.88) sodium chloride solution was injected at the same injection rate. Since the production rate was very low and the injected volume of the high concentration fluid is small, the collected fluid from the wells was diluted and then the conductivity was measured. The concentration of the produced fluid was calculated based on the conductivity of the resulting fluid. Since the produced fluid in well No.4 is almost negligible, no meaningful data was collected for well No.4. Figure 12 shows the calculated concentration of the produced fluid. From this figure, we notice that the concentration peak for well No.2 occurred at t=1636.5 s with the peak value of 53115 PPM. For well No.1, the peak value is 45309 PPM and it occurred at t=1726.5 s. The test was stopped before we got the peak point in well No.3. Since we cannot obtain the realtime concentration of the produced fluid during the test, it was calculated after the circulation test was finished. The injection pressure was also plotted in Figure 12. It shows there was no pressure drop during the test, which indicates no new fracture were generated during the tracer test, so the tracer result can be applied to analyze the geometry of the fracture in the block.

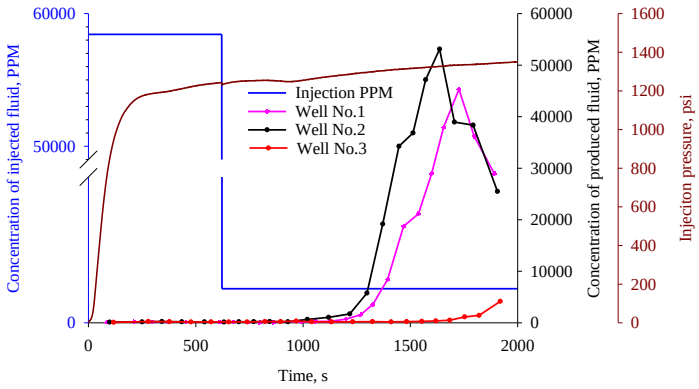

Figure 12: Concentration of the injected and produced fluid and the injection pressure

4. CONCLUSION

We have performed and presented a geothermal reservoir stimulation and production test using 13x13x13 inch^3 pre-heated cubical rock samples under representative in-situ stress regimes. During the stimulation stage, acoustic emissions (AE), pressure and electrical self-potential (SP) were monitored to characterize the induced fracture geometry. The AE cloud and the SP response in the production wells that we obtained agree well with each other; and interpretations from this information agrees with the pressure behavior in the production wells. Following the stimulation stage, cold water was injected centrally and simultaneously collected from nearby production wells. Temperature in the wells and the block surfaces was recorded and production rates were also collected. The maximum temperature drop was as high as 39.22 ^{o}C in the injection well and more than 10 ^{o}C in the production wells. A tracer test was carried out after the circulation test without creating new fractures. The data obtained suggests that for tracer testing a longer test period is needed to obtain the complete full curve of the concentration of the produced fluid. All this information provides concrete data for future fracture properties characterization.

ACKNOWLEDGEMENTS

This project was supported by the U.S. Department of Energy Office of Energy Efficiency and Renewable Energy under Cooperative Agreement DE-EE0006765.0000. This support does not constitute an endorsement by the U.S. Department of Energy of the views expressed in this publication.

REFERENCES

Fitterman D V. 1978. Electrokinetic and magnetic anomalies associated with dilatant regions in a layered earth. Journal of Geophysical Research: Solid Earth. 83(B12): 5923-5928.

Hubbert, M.K. and Willis, D.G. 1957. Mechanics of Hydraulic Fracturing. *Transactions of AIME*. 153-166.

Ishido, T., and Pritchett, J. W. 2003. Characterization of fractured reservoirs using continuous self-potential measurements. *In Proc. 28th Workshop on Geothermal Reservoir Engineering*. 158-165

Ishibashi T, Watanabe N, Hirano N, et al. 2012. Experimental and Numerical Evaluation of Channeling Flow in Fractured Type of Geothermal Reservoir. *Thirty-Seventh Workshop on Geothermal Reservoir Engineering*, Stanford University, Stanford, California.

Jouniaux L, and Pozzi J P. 1995. Streaming potential and permeability of saturated sandstones under triaxial stress: Consequences for electrotelluric anomalies prior to earthquakes. *Journal of Geophysical Research: Solid Earth*. 100(B6): 10197-10209.

Moore, J.R., and Glaser, S.D. 2007. Self-potential observations during hydraulic fracturing. *Journal of Geophysical Research: Solid Earth* 112.B2.

Morgan, F. D. 1989. Fundamentals of streaming potentials in geophysics: Laboratory methods. *In Detection of subsurface flow phenomena*. Springer Berlin Heidelberg. 133-144

MIT-Led Report. 2006. The Future of Geothermal Energy, ISBN: 0-615-13438-6.

Pritchett, J. W., and Ishido, T. 2005. Hydrofracture characterization using downhole electrical monitoring. *In Proceedings of World Geothermal Congress*, Turkey.

Yang Y, Zhang L, Lv J, et al. 2012. Experimental study on fracture process of concrete by acoustic emission technology. *Przegląd Elektrotechniczny*. 88(9b): 55-58.

Hu L, Ghassemi A, et al. 2016. Laboratory Scale Investigation of Enhanced Geothermal Reservoir Stimulation. Forty first Workshop on Geothermal Reservoir Engineering, Stanford University, Stanford, California, February 22-24, 2016